# Contents

# Chapter 7

# The Nucleon-Nucleon Interaction

## 7.1 Scales and relevant degrees of freedom

The degrees of freedom (dofs) which are meaningful in order to describe a physical system are in general determined by the scales which appear in this system. A solid state is for instance described in terms of atoms or molecules and electrons rather than by nuclei, electron shells and electrons. In nuclear physics the situation is similar. In the previous sections we learned that the nucleon substructure can be resolved in deep inelastic scattering experiments with momentum transfer $q^2 > 1$ GeV. This means that short wavelength probes are necessary to *see* quarks and gluons, as illustrated in Fig. 8.3. The wave length of the exchange photon must be essentially smaller then the nucleon radius of $R \sim 1.5$ fm.

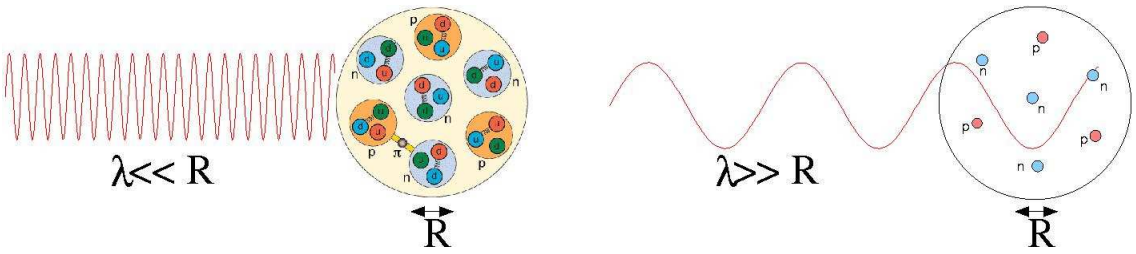


Figure 7.1: Short wave length probes are necessary to resolve quarks and gluons (left) while in low energy physics corresponding to long wave lengths nucleons and mesons are the elementary degrees of freedom (right). (Figure from [1]).

Nuclear physics, i.e. the interaction between nucleons in a bound nucleus or inside neutron stars takes, however, place on a much smaller scale of about $q^2 \sim 0.1$ GeV. Hence the nuclear substructure is not resolved anymore and the relevant degrees of freedom to describe nuclear interactions are nucleons ($qqq$), i.e. protons and neutrons, as elementary particles and mesons ($\bar{q}q$). In nuclear physics mesons play the role of exchange bosons which mediate

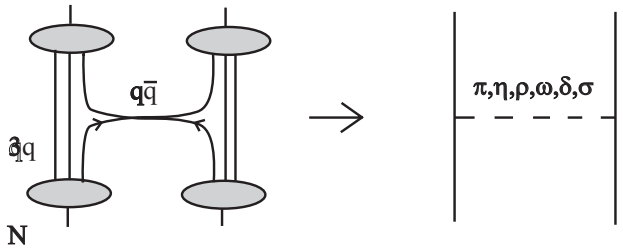


Figure 7.2: Schematic representation of the One-Boson-Exchange model for the nucleon-nucleon interaction. (The figure is taken from [2]).

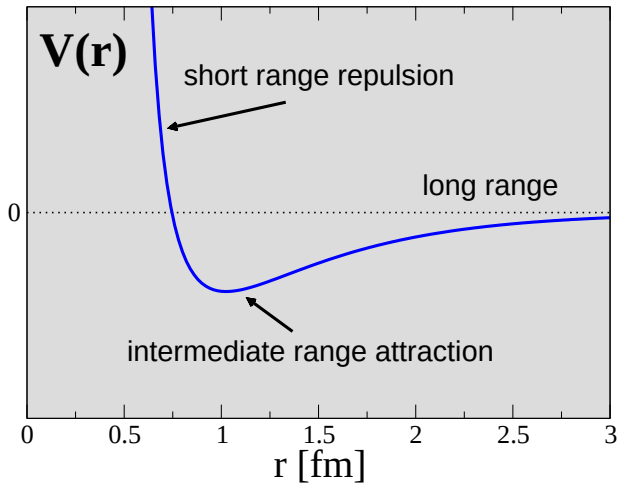


Figure 7.3: Schematic representation of the nucleon-nucleon potential as a function of the relative distance.

the nuclear forces. They act analogous to the photon in QED, with the difference that mesons are massive particles.
Therefore the effective degrees of freedom with which we will deal in the following are nucleons and mesons (see Fig. 7.2). The nucleon-nucleon potential has a Van-der-Waals like structure. It consists of a short-range repulsive part, the so-called *hard core*, an intermediate range attractive part and a long-range part. Schematically this potential is displayed in Fig. 7.3. In the following we will construct this potential as the superposition of the exchange of various mesons of different type.
We start this discussion with the lightest meson, namely the pion.

# 7.2 Pion-Nucleon Interaction

Literature: Ericson and Weise,
**Pions and Nuclei**
Clarendon Press, 1988

## 7.2.1 Structure of pions and nucleons

The pion has a mass of 138 MeV and is the lightest existing meson. The pion is an isospin $I = 1$ particle and exists in three different charge states $(\pi^-, \pi^0, \pi^+)$. For the definition of the *isospin* see Appendix C. Due to its small mass, respectively the long wave length, the pion is responsible for the long range part of the nuclear interactions.

In the previous sections we have seen that the nucleon has an internal structure. As a consequence, the nucleon form factor is not equal to unity. In analogy to the nucleon, pions are not point-like particles as well and therefore the pion form factor is $F_\pi \neq 1$. In the following the form factor will be deduced by applying electron scattering.

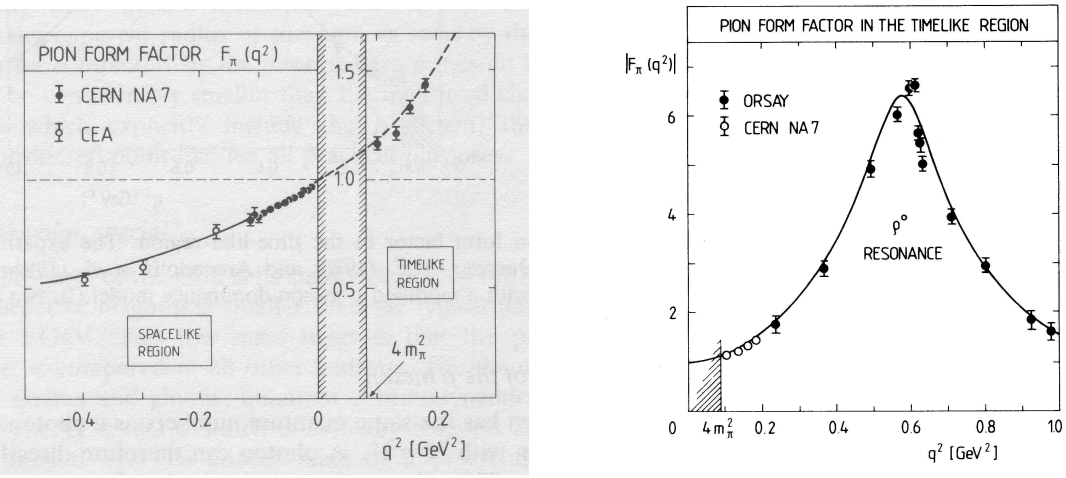


Figure 7.4: Pion form factor in the space-like ($q^2 < 0$) region (left) and in the time-like ($q^2 > 0$) region (right). The region from $0 < q^2 < (2m_\pi)^2$ is kinematically forbidden. (The figures are from [**?**]).

First of all, we discuss shortly two different types of scattering processes which explore the form factor in different regions of momentum transfer, namely the space-like and the time-like region with momentum transfer $q^2 < 0$ and $q^2 > 0$, respectively.

**Electron scattering**

$e^- \pi^\pm \rightarrow e^- \pi^\pm$

$q^2 < 0$

space-like energy-momentum transfer

$\Downarrow$

The form factor is

$$F_\pi(q^2) = 1 + \frac{1}{6} q^2 \langle r_\pi^2 \rangle$$

where the pion radius is

$$\sqrt{\langle r_\pi^2 \rangle} = 0.66 fm$$

being small compared to the nuclear length scale of $1.8 fm$.

**Pair annihilation**

$e^+ e^- \rightarrow \pi^+ \pi^-$

$q^2 > 0$

time-like energy-momentum transfer

$\Downarrow$

resonance structure

$$F_\pi(q^2) = \frac{m_\rho^2}{m_\rho^2 - q^2 - im\Gamma_\rho(q^2)}$$

(see discussion below)

As can be seen from Fig. 7.4 the experimental data of the pion form factor show a clear resonance structure in the time-like region. Such a resonance structure indicates the existence of an unstable particle, namely the resonance, which decays to two pions with high probability. This resonance is the so-called $\rho$-meson which we will meet again in connection with nuclear forces. The $\rho$-meson has a mass of $m_\rho = 770$ MeV and a width of about $\Gamma_\rho = 150$ MeV. Due to the $\rho$ decay $\rho \mapsto \pi\pi$ the form factor has a kinematically forbidden area with $0 \leq q^2 \leq 4m_\pi^2$. The form factor in the spatial region measures the finite size of the pion.
This findings lead to the vector meson dominance model introduced in the following.

**Vector-Meson-Dominance (VMD) Model:**

In this model it is assumed that the photon couples to a pion via an intermediate $\rho$- meson exchange. The $\rho$- meson is a vector meson which means that it is a vector boson like the photon, however, massive. The $\rho$- meson plays also a role in the nucleon-nucleon interaction and there we will discuss its properties in more detail. In any case, this assumption is very successful in the description of the photon-hadron interaction at low energies. The VMD model is therefore not restricted to the pion-photon vertex but it applies also to the photon coupling to other hadrons. We will not go into further details here.
The pion form factor, deduced by using VMD, can be written as

$$F_\pi(q^2) = \frac{m_\rho^2}{m_\rho^2 - q^2 - im\Gamma_\rho(q^2)}$$

where $m_\rho = 770 MeV$ and $\Gamma_\rho = 150 MeV$ is the decay width of the $\rho$. The $\rho$ is unstable and it decays with almost 100% probability into two pions $\rho^0 \rightarrow (\pi^+\pi^- ; \pi^0\pi^0)$.

**Remark**

The $\rho$ has also other decay channels, e.g. that into an electron-positron pair $\rho^0 \rightarrow e^+e^-$ which has a probability of $4.5 \cdot 10^{-5}$. This channel is, however, very important in present research since it allows to study the modifications of the $\rho$ properties in a dense nuclear medium by detecting the electron-positron pairs from $\rho$ decays which were created in heavy ion collisions. There are several large scale experiments at the heavy ion accelerators at CERN (Geneva), RHIC (Brookhaven) and GSI (Darmstadt) devoted to this subject.

---

An equal situation is given for nucleons. The inner structure leads to the nucleon form factor. At moderate $q^2$ the VMD model is also valid in the case of the nucleon. Nucleons are spin $\frac{1}{2}$ particles with an electric and magnetic form factor $G_{E/M}(q^2)$. The electric form factor can to high accuracy be approximated by a dipol form factor

$$G_E(q^2) \approx \frac{1}{\left(1 - \frac{q^2}{\Lambda^2}\right)}$$

where $\Lambda = 0.84GeV$. The charge distribution can be written as the Fourier transform of the electric form factor.

$$\rho_E(r) = \frac{1}{(2\pi)^3} \int d^3q \, e^{i\vec{q}\cdot\vec{r}} G_E(\vec{q}^{\,2}) = \frac{\Lambda^3}{8\pi} e^{-\Lambda r}$$

Note that this picture is valid only at low-energy electron-proton interaction ($-\vec{q}^{\,2} << 1$) which means elastic proton scattering. At higher energies, structure functions (see Sec (**??**)) have to be applied.

### 7.2.2 The free-pion field

The pion is a (pseudo)-scalar particle, because of that the Klein-Gordon equation is satisfied

$$\left(\Box + m_\pi^2\right) \pi_\lambda = 0 \tag{7.1}$$

where $\lambda = \pm 1 \, , 0$ are the different charge states of the pion (see Appendix C).
To solve Eq. (7.1), the free pion Green function or propagator $D(x-y)$ is introduced by

$$\left(\Box_x + m_\pi^2\right) D(x-y) = -\delta^{(4)}(x-y) \, . \tag{7.2}$$

The Green function can be written as

$$D(x-y) = \int \frac{d^4q}{(2\pi)^4} D(q^2) e^{-iq\cdot(x-y)}$$

with

$$D(q^2) = \frac{1}{q^2 - m_\pi^2 + i\epsilon}$$

The poles of $D(q^2)$ are

$$q^2 - m_\pi^2 = \omega^2 - \vec{q}^{\,2} - m_\pi^2 = 0 \; .$$

This condition is satisfied by real particles, so-called on-shell pions:

$$\omega = \pm\sqrt{m_\pi^2 + \vec{q}^{\,2}} \quad \text{where} \left\{ \begin{array}{ll} + & \text{stands for } \pi^+ \\ - & \text{stands for } \pi^- \end{array} \right. .$$

(Since $\pi^0$ is its own antiparticle, it can have both solutions $\pm$.) Next, virtual or off-shell pions are considered with $q_0 = \omega = 0$. Therefore the pion propagator[1] is independent of time

$$\left(\vec{\nabla}^2 - m_\pi^2\right) G\left(\vec{x} - \vec{y}\right) = \delta^3(\vec{x} - \vec{y}) \; . \tag{7.3}$$

$G\left(\vec{x} - \vec{y}\right)$ becomes

$$G\left(\vec{x} - \vec{y}\right) \; = \; \frac{e^{-m_\pi |\vec{x} - \vec{y}|}}{4\pi \left|\vec{x} - \vec{y}\right|} \tag{7.4}$$

or in polar coordinates

$$\boxed{G(r) \; = \; \frac{e^{-m_\pi r}}{4\pi r}} \tag{7.5}$$

which represents the *Yukawa* potential. The form of this potential is typical for the exchange of massive bosons. Its characteristic range is given by the pion compton wavelength $\lambda = \frac{1}{m_\pi} \approx 1.4 fm$. In momentum-space the pion-propagator is represented by the Fourier transform of $G(\vec{x})$

$$D(-\vec{q}) = \int d^3x \, e^{-\vec{q}\cdot\vec{x}} \, G(\vec{x}) = \frac{-1}{\vec{q}^{\,2} + m_\pi^2} \; . \tag{7.6}$$

### 7.2.3 Pion-nucleon coupling

We consider now first a static pion field with a source term. This is fully analogous to the static photon field generated by the presence of charges. Now the charge is represented by a nucleon which sits at the position $\vec{r}$. Because of the isovector and pseudo-scalar properties of the pion, the coupling to the nucleon is, however, different. The pion field couple to the isospin of the nucleon expressed by the $\tau_3$ matrix and the vertex itself is the so-called pseudoscalar vertex which contains a derivative coupling to the nucleon field. For simplicity we assume that the nucleon is a point-like particle. Hence the static Klein-Gordon equation (7.2) reads by the presence of a source term

$$\left(\vec{\nabla}^2 - m_\pi^2\right) \pi_0(\vec{x}) = \frac{f}{m_\pi} \, \tau_3 \, \vec{\sigma} \cdot \vec{\nabla}_x \delta^{(3)}\left(\vec{x} - \vec{y}\right) = \rho_0(\vec{x}) \tag{7.7}$$

[1] We denote by $D$ the covariant Green function whereas $G$ stands for static propagator.

with the coupling constant $f$. From (7.7) we obtain the solution for the pion field by convoluting the free propagator (7.4) over the source term

$$\pi_0(\vec{x}) = \int d^3y\, G(\vec{x}-\vec{y})\,\rho_0(\vec{x}) = -\frac{f}{m_\pi}\tau_3\vec{\sigma}\cdot\vec{\nabla}_x\frac{e^{-m_\pi|\vec{x}-\vec{r}|}}{4\pi\,|\vec{x}-\vec{r}|} \tag{7.8}$$

$$= f\tau_3\vec{\sigma}\cdot\hat{x}\left(1+\frac{1}{m_\pi|\vec{x}|}\right)\frac{e^{-m_\pi|\vec{x}|}}{4\pi|\vec{x}|} \quad (\text{for } \vec{r}=0)\ . \tag{7.9}$$

**Relativistic Lagrangian**

In (7.7) we introduced the pion-nucleon coupling by hand. It follows from the corresponding pion-nucleon Lagrangian. The relativistic Lagrangian is given by the sum of

$$L = L_0 + L_{WW}$$

where $L_0$ contains the contributions from the free pion and nucleon fields and has the form

$$L_0 = \bar{\psi}\,(i\gamma_\mu\partial^\mu - M)\,\psi + \frac{1}{2}\left(\partial_\mu\vec{\pi}\cdot\partial^\mu\vec{\pi} - m_\pi^2\vec{\pi}^2\right)$$

From $L_0$ the equation of motion for the pion field, i.e. the Klein-Gordon equation (7.2) is obtained by the corresponding Euler-Lagrange equations:

$$\partial^\mu\frac{\partial L}{\partial(\partial_\mu\Phi)} - \frac{\partial L}{\partial\Phi} = 0$$

where $\Phi$ represents a scalar field and $\Phi^\mu$ stands for a vector field.

In the same way the free Dirac equation follows for the nucleon field $\psi$. The interesting part is the interaction term $L_{WW}$ which contains the coupling of the pion to the nucleon field $\psi$. Covariantly the pseudoscalar coupling is given by a $\gamma_5$ matrix. If we express the three different isospin states of the pion by $\vec{\pi}$ (see again Appendix C) the interaction term can be written as

$$\boxed{L_{\pi NN} = i\frac{f}{m_\pi}\bar{\psi}(x)\,\gamma_5\,\vec{\tau}\psi(x)\cdot\vec{\pi}(x)\ .} \tag{7.10}$$

**Remark: Lagrangian of fields**

The following table serves to illustrate the analogy between the Lagrange function in classical mechanics and the Lagrangian for fields in quantum field theory.

| | Particles | Fields |
|---|---|---|
| generalised coordinates | $\vec{q}_i(t)$ | $\Phi(\vec{x},\ t)$ |
| independent variable | $i,\ t$ | $\vec{x},\ t = x_\mu$ |
| Lagrangian | $L\left(\vec{q}_i,\ \dot{\vec{q}}_i\right)$ | $L(\Phi,\ \partial_\mu \Phi)$ |
| Euler-Lagrange equation | $\frac{d}{dt}\frac{\partial L}{\partial \dot{q}_i} - \frac{\partial L}{\partial q_i} = 0$ | $\partial_\mu \frac{\partial L}{\partial(\partial_\mu \Phi)} - \frac{\partial L}{\partial \Phi} = 0$ |
| $\Rightarrow$ | equation of motion of $\vec{q}_i$ | field equation of $\Phi(x)$ |

---

**Pseudoscalar coupling**

The covariant equation of motion for the $\pi$-field which in its static form was already given in Eq. (7.7) is now obtained by the application of the Euler-Lagrange equations to the full pion-nucleon Lagrangian $L_{\pi NN}$ (7.10) and yields

$$\boxed{\left(\partial_\mu \partial^\mu + m_\pi^2\right)\vec{\pi} \ = \ -i\frac{f}{m_\pi}\bar{\psi}\gamma_5\vec{\tau}\psi} \tag{7.11}$$

In the following we want to see how the $\gamma_5$ matrix in (7.11) transforms into the derivative in (7.7). To do so, we have to evaluate the matrix element $\bar{\psi}\gamma_5\vec{\tau}\psi$. For this purpose we assume that the nucleon has the spin $+\frac{1}{2}$. Inserting the nucleon spinor given by

$$\psi_+ \ = \ \sqrt{E+m}\begin{pmatrix} 1 \\ 0 \\ \frac{\vec{\sigma}\cdot\vec{p}}{E+m} \\ 0 \end{pmatrix} e^{-ip\cdot x} = u(p)e^{-ip\cdot x}$$

we can evaluate

$$\begin{aligned} \bar{\psi}(x)\,\gamma_5\,\psi(x) \ &= \ \bar{u}(p')\,\gamma_5\,u(p)\,e^{-i(p-p')\cdot x} \\ &= \ u^\dagger(p')\,\gamma_0\gamma_5\,u(p)\,e^{-i(p-p')\cdot x}\ . \end{aligned}$$

By inserting $u(p)$ and using the two component Pauli spinor $\chi$, the following expression is obtained

$$\begin{aligned}\bar{\psi}(x)\,\gamma_5\,\psi(x) &= \left(-\chi^\dagger\,\vec{\sigma}\cdot\vec{p}'\,\chi+\chi^\dagger\,\vec{\sigma}\cdot\vec{p}\,\chi\right)\frac{N^2}{\sqrt{E+m}}e^{-i(p-p')\cdot x}\\ &= \frac{N^2}{\sqrt{E+m}}\vec{\sigma}\cdot(\vec{p}-\vec{p}')\,e^{i(\vec{p}-\vec{p}')\cdot\vec{x}}\,.\end{aligned}$$

The Fourier transform leads to

$$FT\left(\frac{N^2}{\sqrt{E+m}}\vec{\sigma}\cdot(\vec{p}-\vec{p}')\,e^{i(\vec{p}-\vec{p}')\cdot\vec{x}}\right)=i\vec{\sigma}\cdot\vec{\nabla}_x\,\delta^{(3)}(\vec{x})\,.$$

*The $\gamma_5$ coupling is equivalent to a derivative coupling after Fourier transformation.*

### 7.2.4 Pion exchange potential

The strong interaction process is analogous to the electromagnetic interaction. Whereas the electrodynamic interaction is based on photon exchange, mesons play the role of exchange bosons in nuclear physics. These are effective degrees of freedom for the description of the low-energy sector of QCD. As already mentioned, the pion is the lightest of them with mass $m_\pi = 138$ MeV. For this reason it is responsible for the longest-range part of the nucleon-nucleon interaction with a range of $\lambda \sim 1.4$ fm.
A pion field generated by a point-like nucleon, located at $\vec{r}_1$ with spin $\frac{1}{2}$ and isospin $\frac{1}{2}$, is described by

$$\vec{\pi}(\vec{x})=-\frac{f}{m_\pi}\vec{\tau}_1\left(\vec{\sigma}_1\cdot\vec{\nabla}_x\right)\frac{e^{-m_\pi|\vec{x}-\vec{r}_1|}}{4\pi\,|\vec{x}-\vec{r}_1|}$$

and the source function given by

$$\vec{\rho}(\vec{x})=\frac{f}{m_\pi}\vec{\tau}_1\left(\vec{\sigma}_1\cdot\vec{\nabla}_x\right)\delta^{(3)}(\vec{x}-\vec{r}_1)\,.$$

The spin and isospin matrices $\vec{\sigma}_1$ and $\vec{\sigma}_2$ refer to the nucleon and act on the nucleon wave function. Now, we introduce a second nucleon located at position $\vec{r}_2$. The interaction energy between the second nucleon and the pion field generated by the first nucleon is now obtained by integrating the pion field over the source term of nucleon 2 as schematically displayed in Fig. 7.5:

$$V_\pi(\vec{r}_1,\ \vec{r}_2)=\int d^3x\,\vec{\rho}_2(\vec{x})\cdot\vec{\pi}(\vec{x})$$

Inserting the relative distance $\vec{r}=\vec{r}_1-\vec{r}_2$ the static one-pion exchange potential is obtained

$$\boxed{V_\pi(\vec{r})=\frac{f^2}{m_\pi^2}\vec{\tau}_1\cdot\vec{\tau}_2(\vec{\sigma}_1\cdot\vec{\nabla})(\vec{\sigma}_2\cdot\vec{\nabla})\frac{e^{-m_\pi r}}{4\pi r}} \tag{7.12}$$

This expression is very similar to the magnetic dipole-dipole interaction potential.

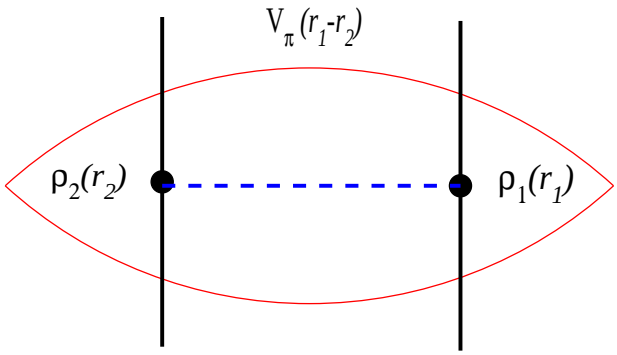


Figure 7.5: Schematic representation of the One-Pion-Exchange potential.

**Decomposition of $V_\pi$ into central potential and tensor term**

The structure of the potential given by Eq. (7.12) is not yet very transparent since the gradients act on the Yukawa term at the right of (7.12). Now we want to separate the different contributions in $V_\pi$ in a more transparent form and to write it as the sum of a central and tensor potential. To do so, we write

$$(\vec{\sigma}_1 \cdot \vec{\nabla})(\vec{\sigma}_2 \cdot \vec{\nabla}) = \frac{1}{3}(\vec{\sigma}_1 \cdot \vec{\sigma}_2)\vec{\nabla}^{\,2} + \frac{1}{3}\left[3(\vec{\sigma}_1 \cdot \vec{\nabla})(\vec{\sigma}_2 \cdot \vec{\nabla}) - (\vec{\sigma}_1 \cdot \vec{\sigma}_2)\,\vec{\nabla}^{\,2}\right]$$

The derivatives can be evaluated:

$$\vec{\nabla}^{\,2}\frac{e^{-\mu r}}{r} = \mu^2\frac{e^{-\mu r}}{r} - 4\pi\delta^{(3)}(\vec{r})$$

$$\left(\vec{\sigma}\cdot\vec{\nabla}\right)\frac{e^{-Mr}}{r} = \left[-M\vec{\sigma}\cdot\hat{r} - \frac{1}{r}\vec{\sigma}\cdot\vec{r}\right]\frac{e^{-Mr}}{r}, \quad \text{where } \hat{r} = \frac{\vec{r}}{r} \quad .$$

Now we introduce the *tensor operator*

$$\boxed{\hat{S}_{12}(\hat{r}) := 3(\vec{\sigma}_1 \cdot \hat{r})(\vec{\sigma}_2 \cdot \hat{r}) - \vec{\sigma}_1 \cdot \vec{\sigma}_2} \tag{7.13}$$

Inserting the above expressions into Eq.(7.12) we obtain now a transparent representation of the one-pion-exchange potential

$$\boxed{\begin{aligned} V_\pi(\vec{r}) = {} & \frac{1}{3}\frac{f^2}{4\pi}\left[\frac{e^{-m_\pi r}}{r} - \frac{4\pi}{m_\pi^2}\delta^{(3)}(\vec{r})\right]\vec{\sigma}_1\cdot\vec{\sigma}_2\;\vec{\tau}_1\cdot\vec{\tau}_2 \\ & + \underbrace{\frac{1}{3}\frac{f^2}{4\pi}\left(1 + \frac{3}{m_\pi r} + \frac{3}{m_\pi^2 r^2}\right)\frac{e^{-m_\pi r}}{r}\hat{S}_{12}(\hat{r})\vec{\tau}_1\cdot\vec{\tau}_2}_{\textit{tensor term}} \end{aligned}} \tag{7.14}$$

The first term represents the central potential which is of Yukawa type. The second term proportional to the $\delta$-function represents a zero-range contact potential. Both are supplemented by the spin-isospin matrices acting on the nucleon wave functions.
The tensor term is a novel feature of the pion exchange which has no analog in the photon exchange. It has, however, an analog in electrodynamics, namely the magnetic dipole-dipole interaction. Comparing the pion interaction potential (7.12) to the magnetic dipole-dipole interaction

$$V_{\mu\mu} = \underbrace{-\frac{2}{3}\vec{\mu}_1 \cdot \vec{\mu}_2 \delta^{(3)}(\vec{r})}_{\text{contact term}} \underbrace{- \frac{3(\vec{\mu}_1 \cdot \hat{r})(\vec{\mu}_2 \cdot \hat{r}) - \vec{\mu}_1 \cdot \vec{\mu}_2}{4\pi r^3}}_{\text{tensor term}}$$

we find the following similarities:

- Whereas the magnetic dipole interaction is based on a transversal coupling $\vec{\sigma} \times \vec{\nabla}$, the axial $\pi$ dipole interacts via a so-called longitudinal coupling $\vec{\sigma} \cdot \vec{\nabla}$.
- Both interaction potentials include a contact term, which results from the idealised point-like particles, acting as sources.
- The pion potential contains the Yukawa potential. In contrast, the magnetic potential includes no corresponding term. This is caused by the finite pion mass whereas photons are massless.

**Spin-isospin structure of the one-pion exchange**

Next we want to consider the spin-isospin structure of the one-pion-exchange (OPE) in more detail. To do so, we consider the possible wave functions for two nucleons coupled to total spin $S = s_1 + s_2 = 0,\ 1$ with $s_1 = s_2 = \frac{1}{2}$:

$$S = 0 \qquad \tfrac{1}{\sqrt{2}}\left(\left|\tfrac{1}{2}\ -\tfrac{1}{2}\right\rangle - \left|-\tfrac{1}{2}\ \tfrac{1}{2}\right\rangle\right) \quad S_z = 0 \qquad \text{Singlet (anti-symmetric)}$$

$$S = 1 \qquad \left\{ \begin{array}{ll} \left|-\tfrac{1}{2}\ -\tfrac{1}{2}\right\rangle & S_z = -1 \\ \tfrac{1}{\sqrt{2}}\left(\left|\tfrac{1}{2}\ -\tfrac{1}{2}\right\rangle + \left|-\tfrac{1}{2}\ \tfrac{1}{2}\right\rangle\right) & S_z = 0 \\ \left|\tfrac{1}{2}\ \tfrac{1}{2}\right\rangle & S_z = 1 \end{array} \right\} \qquad \text{Triplet (symmetric) .}$$

The total OPE potential has to be anti-symmetric. Since the potential depends only on the relative distance $|\vec{r}| = |\vec{r}_1 - \vec{r}_2|$, the spatial part of the pion-exchange is symmetric under exchange of particle 1 and 2. Therefore the spin-isospin-angular momentum dependent part of the potential has to be antisymmetric. This leads to the *selection rule*

$$S + I + L = J + I = \text{odd} \,. \tag{7.15}$$

For further evaluation we consider the spin-isospin matrix elements. In spin-isospin space the two nucleons can occur in a singlet-singlet ($S = 0, I = 0$), a triplet-triplet ($S = 1, I = 1$) or in a mixed singlet-triplet state. The spin-isospin coefficients are easily obtained from $\vec{s}_1 \cdot \vec{s}_2 = \frac{1}{2}[\vec{S}^2 - \vec{s}_1^{\,2} - \vec{s}_2^{\,2}]$ with $\vec{s} = \frac{1}{2}\vec{\sigma}$:

$$\langle S|\vec{\sigma}_1 \cdot \vec{\sigma}_2|S\rangle = [2(S+1)S - 3] \tag{7.16}$$

and anlogously for the isospin. Hence the spin-isospin operators lead for the various cases to the following coefficients:

$$\langle SI|\vec{\sigma}_1 \cdot \vec{\sigma}_2 \; \vec{\tau}_1 \cdot \vec{\tau}_2|SI\rangle = 4\left[(S+1)S - \frac{3}{2}\right]\left[(I+1)I - \frac{3}{2}\right]$$

$$= \begin{cases} 9 & S = I = 0 \\ 1 & S = I = 1 \\ -3 & (S,\, I) = (1,\, 0),\ (0,\, 1) \end{cases}$$

Furthermore the tensor term (7.13) vanishes in the spin-singlet, i.e. $S_{12}(\hat{r})|S = 0\rangle$ (see below). As a consequence, the tensor term is only relevant in the spin-triplet state. Due to the selection rule (7.15) the possible spin-isospin combinations are determined by the value of the total angular momentum $L$ of the two nucleons. In summary we have

$$\begin{aligned}
V_\pi(S = I = 0,\ L \text{ odd}) &= \frac{3f^2}{4\pi}\frac{e^{-m_\pi r}}{r} \\
V_\pi(S = 0,\ I = 1,\ L \text{ even}) &= -\frac{f^2}{4\pi}\frac{e^{-m_\pi r}}{r} \\
V_\pi(S = I = 1,\ L \text{ odd}) &= \frac{1}{3}\frac{f^2}{4\pi}\left[1 + \left(1 + \frac{3}{m_\pi r} + \frac{3}{m_\pi^2 r^2}\right)\hat{S}_{12}(\hat{r})\right]\frac{e^{-m_\pi r}}{r} \\
V_\pi(S = 1,\ I = 0,\ L \text{ even}) &= -\frac{f^2}{4\pi}\left[1 + \left(1 + \frac{3}{m_\pi r} + \frac{3}{m_\pi^2 r^2}\right)\hat{S}_{12}(\hat{r})\right]\frac{e^{-m_\pi r}}{r}\,.
\end{aligned}$$

Thus the OPE has a very complex structure of different values and even different signs (!) in different partial waves and for different spin-isospin combinations. This is a genuine new feature of the nucleon-nucleon interaction!

---

**Auxiliary calculation**

We show that

$$\hat{S}_{12}|S = 0\rangle = 0 \quad \text{(singlet)}\,.$$

By choosing $\hat{r} = \hat{e}_z$, Eq. (7.13) becomes

$$\hat{S}_{12}|S = 0\rangle = \left(3\sigma_z^{(1)}\sigma_z^{(2)} - [2(S+1)S - 3]\right)|S = 0\rangle = 3[\sigma_z^{(1)}\sigma_z^{(2)} + 1]|S = 0\rangle$$

and therefore

$$\hat{S}_{12}|S=0\rangle = \frac{3}{\sqrt{2}}\left[-\left|\frac{1}{2}\ -\frac{1}{2}\right\rangle + \left|-\frac{1}{2}\ \frac{1}{2}\right\rangle + \left|\frac{1}{2}\ -\frac{1}{2}\right\rangle - \left|-\frac{1}{2}\ \frac{1}{2}\right\rangle\right] = 0\ .$$

---

An interesting question is now, in which kinematical regimes which part of the interaction, i.e. central or tensor part, is more important? By substituting $x = m_\pi r$, the central potential takes the form

$$V_\pi^C = \propto \frac{f^2}{4\pi}\frac{e^{-x}}{x}\ .$$

The tensor term can be written by

$$V_\pi^T \propto \frac{f^2}{4\pi}\left(1+\frac{3}{x}+\frac{3}{x^2}\right)\ \frac{e^{-x}}{x}\ .$$

In the limit $x \mapsto 0$ the ratio $\frac{V_\pi^T}{V_\pi^C}$ goes like $\lim_{x\mapsto 0}\frac{V_\pi^T}{V_\pi^C} = 1/x^2$. With $m_p i \sim 0.7$ fm$^{-1}$ follows that $rm_\pi < 1$ for $r < 0.7$ fm which shows that for the short range part the one-pion exchange is totally dominated by the tensor force. However, even at intermediate distances the tensor force is enhanced by the factor of 3 of the $1/x$ term.

For completeness we show finally the momentum-space representation of the OPE which is obtained after Fourier transformation. It reads

$$\boxed{V_\pi(\vec{q}) = -\frac{1}{3}\frac{f^2}{m_\pi^2}\left[\left(1-\frac{m_\pi^2}{\vec{q}^{\,2}+m_\pi^2}\right)\ \vec{\sigma}_1\cdot\vec{\sigma}_2 + \frac{\vec{q}^{\,2}}{\vec{q}^{\,2}+m_\pi^2}\hat{S}_{12}(\hat{q})\right]\ \vec{\tau}_1\cdot\vec{\tau}_2}$$

The first term in the bracket corresponds to the contact term in coordinates space $\delta^{(3)}(\vec{x})$ (see Eq. (7.14)), the second term with the propagator originates from the central potential $V_\pi^C$ (the Yukawa potential) and the third term represents the tensor part $V_\pi^T$. If zero momentum transfer, i.e. $\vec{q}=0$, $V_\pi^T$ is equal to zero.

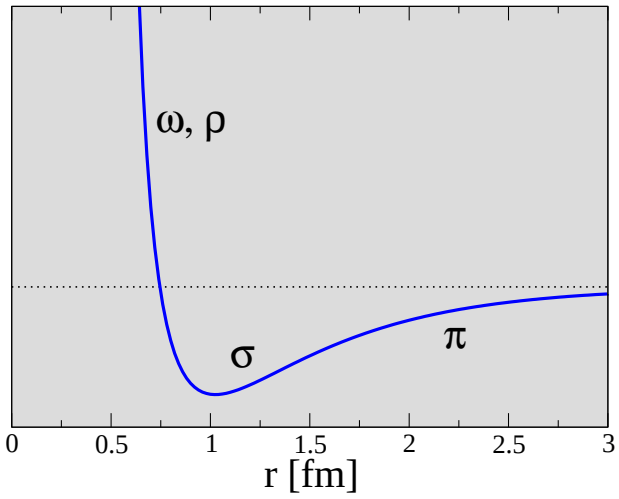


Figure 7.6: Schematic representation of the two-nucleon potential (central part) generated by the exchange of different mesons. $r$ denotes the relative distance of the two nucleons.

## 7.3 Boson exchange potentials

The nucleon-nucleon (NN) interaction has a complex structure as schematically depicted in Fig. 7.6. The central part of the nucleon-nucleon potential consists of a short range repulsive part, an intermediate range attractive and a long range part. In modern relativistic potentials based on field theory this interaction is described by the exchange of various mesons which act as exchange bosons. The most important are the non-strange mesons $\pi$, $\rho$, $\omega$ and $\sigma$.
The previous section was devoted to the discussion of the pion exchange which is responsible for the long range interaction. Now we extend the discussion to the other mesons. Hence the total NN-interaction is given by the superposition of the contributions from the various mesons. These contributions are characterised by the coupling strength $g_i$, the meson mass $m_i$ and the character of the meson which determines the Lorentz structure of the meson-nucleon vertex $\Gamma_i$ (scalar, vector, ...). To summarise:

| | | |
|---|---|---|
| Coupling strength: | $g_i$ with sign $\left\{ \begin{array}{ll} \text{attractive} & + \\ \text{repulsive} & - \end{array} \right.$ | |
| Meson mass: | $m_i$ determines the range | |
| Meson-nucleon vertex: | $\Gamma_i$ determines the Lorentz structure | |

First of all we give a short overview of the different mesons and the corresponding coupling properties:

- $\pi$-meson:
  $m_\pi = 138$ MeV, spin S=0, isospin I=1

pseudoscalar coupling where the tensor force is the most important part
long range interaction

$$L_{\pi NN} = \frac{f}{m_\pi}\bar{\psi}(x)\, i\gamma_5\, \vec{\tau}\, \psi(x)\bar{u}(x)$$

- $\sigma$-meson:
  $m_\sigma \approx 550MeV$, S=0, I=0
  scalar coupling, attractive
  intermediate range interaction

$$L_{\sigma NN} = g_\sigma \bar{\psi}\mathbb{1}\psi\Phi(x)$$

- $\omega$-meson:
  $m_\omega = 783$ MeV, S=1, I=0
  vector coupling, repulsive
  short range interaction

$$L_{\omega NN} = -g_\omega \bar{\psi}(x)\, \gamma_\mu \psi(x)\omega^\mu(x)$$

- $\rho$-meson:
  $m_\rho = 770$ MeV, S=1, I=1
  vector and tensor coupling
  short range interaction

$$L_{\rho NN} = -g_\rho \bar{\psi}(x)\, \gamma_\mu\, \vec{\tau}\, \psi(x)\, \vec{\rho}^{\,\mu}(x) + \frac{g_\rho^T}{2M}\bar{\psi}(x)\, \sigma_{\mu\nu}\, \vec{\tau}\, \psi(x)\, \partial^\nu\, \vec{\rho}^{\,\mu}(x)$$

Mesons with isospin $I = 1$ are isovector particles and couple to the isospin of the nucleon, i.e. they distinguish between protons and neutrons, mesons $I = 0$ are isoscalar and do not distinguish. The $\rho$-meson has a vector coupling $\gamma_\mu$ and a tensor coupling $\sigma_{\mu\nu}\partial^\nu$. The pion-nucleon coupling strength $f$ is determined by some fundamental QCD relations (Effective chiral QCD Lagrangian). For all other mesons the coupling strengths $g_i$ are fixed from empirical nucleon-nucleon scattering data. For the $\rho$ this implies a relation $g_\rho^T \sim 6g_\rho$.
Modern Boson-Exchange potentials describe NN-scattering data with high precision. Such potentials were developed in the mid-eighties. Typcal examples are the so-called Bonn and Nijmegen potentials developed by the Bonn-Jülich [4] and the Nijmegen (Netherlands) [5] research groups. In addition to the mesons discussed above such potentials contain in addtion an isoscalar pseudoscalar meson, the so-called $\eta$-meson, and an isovector scalar meson, the so-called $\delta$-meson. Thus they are based on a complete set of non-strange mesons (mesons which have no strange quark content) with masses below 1 GeV. The model parameters, i.e. the meson-nulceon coupling strenghts (and additional parameters for form factors) are fitted to NN-scattering data (about 3000 data points for proton-proton and proton-neutron scattering) and the achieved precision is a $\chi^2$ per datum of about $1.8 \div 1.9$. More recent version like CD-Bonn [6] reach even a $\chi^2$ per datum of about $1.01 \div 1.02$.

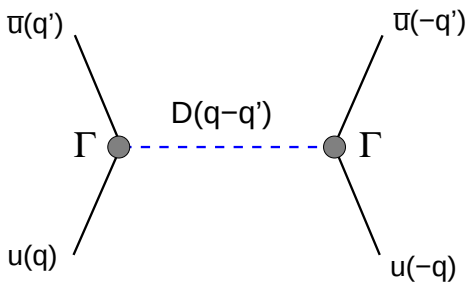


Figure 7.7: Schematic representation of the one-boson exchange diagram.

**Spin-structure of one-boson-exchange potentials**

An expansion in $\frac{1}{M}$ to leading order yields the non-relativistic form of the scalar and vector potentials.

1. Scalar potential, generated by the $\sigma$-meson

$$V_s(\vec{r}) = \underbrace{-\frac{g_s^2}{4\pi}\frac{e^{-m_s r}}{r}}_{\text{attractive central potential}} + \underbrace{\frac{g_s^2}{4\pi}\frac{1}{2M^2r^2}\frac{d}{dr}\left(\frac{e^{-m_s r}}{r}\right)\vec{L}\cdot\vec{S}}_{\text{spin-orbit potential}}$$

   where $\vec{S} = \frac{1}{2}(\vec{\sigma}_1 + \vec{\sigma}_2)$ is the total spin and $\vec{L}$ the total angular momentum of the two-nucleon system.

2. Vector potential, represented by $\omega$- and $\rho$-mesons

$$V_V = \underbrace{\frac{g_V^2}{4\pi}\frac{e^{-m_V r}}{r}}_{\text{repulsive}} + \frac{g_V^2}{4\pi}\left(3 + 4\frac{g_T}{g_V}\right)\frac{1}{2M^2r^2}\frac{d}{dr}\left(3 + 4\frac{g_T}{g_V}\right)\vec{L}\cdot\vec{S}$$
$$+ \underbrace{\frac{g_V^2}{4\pi}\left(1 + \frac{g_T}{g_V}\right)^2\frac{m_V^2}{4\pi}\left(\vec{\sigma}_1\times\vec{\nabla}\right)\left(\vec{\sigma}_2\times\vec{\nabla}\right)\frac{e^{-m_V r}}{r}}_{\text{tensor force, transversal coupling}} .$$

### 7.3.1 Momentum space representation of the OBE potentials

We want now first to evaluate the Feynman-diagram which corresponds to a one-meson exchange. For the moment we disregard the isospin. In the two-nucleon center-of-mass system the incoming nucleons have momenta $\pm\vec{q}$, the outgoing nucleons have momenta $\pm\vec{q}\,'$. The nucleons are on-shell and therefore we have

$$E = \sqrt{M^2 + \vec{q}^{\,2}} \quad \text{and} \quad E' = \sqrt{M^2 + \vec{q}^{\,\prime 2}} \, .$$

Since we consider only elastic scattering, energy-momentum conservation implies

$$|\vec{q}\,'| = |\vec{q}| \qquad \text{and} \qquad E = E' \; .$$

Applying the Feynman rules for evaluating the meson exchange potential $V_\alpha(\vec{q},\vec{q}')$ where the index $\alpha$ stands for the various types of possible mesons exchanged $\alpha = \pi,\ \sigma,\ \rho,\ \cdots$, one finds

$$\boxed{V_\alpha = g_1 \bar{u}_1(\vec{q}\,')\Gamma_1\, u_1(\vec{q})\, D_\alpha(q-q')\, g_2\, \bar{u}_2(-\vec{q}\,')\Gamma_2\, u_2(-\vec{q})} \tag{7.17}$$

$D_\alpha$ in (7.16) represents the meson propagator. The meson propagator is different for (pseudo)-scalar and vector particles and reads

$$D_\alpha = \frac{P_\alpha}{(q-q')^2 - m_\alpha^2} \; .$$

where $P_\alpha$ depends on the type of interchanged meson:

$$P_\alpha = \begin{cases} \mathbb{1} & \text{(pseudo) scalar meson:} \quad \sigma,\ \pi \\ -g^{\mu\nu} & \text{vector meson:} \qquad\quad \omega,\ \rho \end{cases} \; .$$

The $\Gamma_{1,2}$ matrices are the so-called vertex-functions or meson-nucleon couplings which are given by

| Particle: | $\sigma-$meson | Pion | $\omega-$meson |
|---|---|---|---|
| $\Gamma$ : | $\mathbb{1}$ | $\gamma_5$ | $\gamma^\mu$ |

We now give a basic example to illustrate our findings. Consider the case that a scalar meson ($\sigma$) is exchanged. This is the simplest example, but the other amplitudes can be evaluated in an analogous way. We discuss elastic, i.e. on-shell scattering with $E = E'$ . In this case $V_\sigma$ becomes

$$V_\sigma(\vec{q}) = g_\sigma^2\, \frac{\bar{u}_1(\vec{q}\,')\, u_1(\vec{q})\, \bar{u}_2(-\vec{q}\,')\, u_2(-\vec{q})}{-(\vec{q}\,'-\vec{q})^2 - m_\sigma^2} \; .$$

To compute $V_\sigma$, we use

$$\begin{aligned} \bar{u}_1(\vec{q}\,')u_1(\vec{q}) &= u_1^\dagger(\vec{q}\,')\,\gamma_0\, u_1(\vec{q}) \\ &= \sqrt{\frac{(E'+M)\,(E+M)}{4E'E}}\, \left(1,\ \frac{-\vec{\sigma}\cdot\vec{q}\,'}{E'+M}\right) \begin{pmatrix} 1 \\ \frac{\vec{\sigma}\cdot\vec{q}}{E+M} \end{pmatrix} \\ &= \frac{E+M}{2E}\, \left(1 - \frac{\vec{q}\,'\cdot\vec{q} + i\,\vec{\sigma}_1\cdot(\vec{q}\,'\times\vec{q})}{(E+M)^2}\right) \end{aligned}$$

and we insert following relation

$$(\vec{\sigma}\cdot\vec{a})(\vec{\sigma}\cdot\vec{b}) = \vec{a}\cdot\vec{b} + i\,\vec{\sigma}\cdot(\vec{a}\times\vec{b}) \; .$$

**Auxiliary calculation:**

$$\begin{aligned}(\vec{\sigma}\cdot\vec{a})(\vec{\sigma}\cdot\vec{b}) &= \left(\sum_i \sigma_i a_i\right)\left(\sum_k \sigma_k b_k\right) = \sum_{i\,k} \sigma_i\sigma_k\, a_i b_k \\ &= \sum_k \sigma_k^2 a_k b_k + \sum_{i\neq k} i\epsilon_{ikm}\sigma_m a_i b_k \\ &= \vec{a}\cdot\vec{b} + i\,\vec{\sigma}\cdot(\vec{a}\times\vec{b})\,.\end{aligned}$$

---

### 7.3.2 Non-relativistic reduction

Now we introduce the momentum transfer

$$\vec{k} \equiv \vec{q}\,' - \vec{q}$$

and the center-of-mass momentum

$$\vec{P} = \frac{1}{2}\,(\vec{q} + \vec{q}\,')\,.$$

The vector product reads in terms of c.m. momentum and momentum trnasfer

$$\vec{n} = \vec{q}\times\vec{q}\,' \equiv \vec{P}\times\vec{k} \quad .$$

Furthermore, in the nonrelativistic limit with $E \cong M$, one obtains

$$E = \sqrt{M^2 + \vec{q}^{\,2}} = M\,(1 + \frac{\vec{q}^{\,2}}{2M} + \cdots)\,.$$

The total matrix element for the scalar $\sigma$ exchange contains two vertices of type $\bar{u}u$ and the meson propagator. The latter is taken in its static form $(-1)/(\vec{k}^2 + m^2)$. Altogethr, this yields in the non-relativistic limit, the scalar potential of form

$$V_\sigma(\vec{k}) = \underbrace{\frac{-g_\sigma^2}{\vec{k}^{\,2} + m_\sigma^2}}_{\text{Yukawa potential}} \left[1 + \frac{\frac{1}{2}(\vec{\sigma}_1 + \vec{\sigma}_2)(-i)\vec{k}\times\vec{P}}{2M^2}\right]\,.$$

We recognize an attractive Yukawa potential and the spin-orbit potential which is the second term in brackets. It corresponds to $O_4$ of the complete operator expansion given below in (**??**).

The complete OBE potentials as e.g. the Bonn potentials can be reduced to a non-relativistic representation by expanding the full field-theoretical OBE Feynman amplitudes into a set of spin and isospin operators

$$V = \sum_i [V_i + V_i' \, \vec{\tau}_1 \cdot \vec{\tau}_2] \; O_i. \tag{7.18}$$

The operators $O_i$ obtained in this low energy expansion, assuming identical particle scattering and charge independence, are defined as

$$\begin{aligned} O_1 &= 1, \\ O_2 &= \vec{\sigma}_1 \cdot \vec{\sigma}_2, \\ O_3 &= (\vec{\sigma}_1 \cdot \vec{k})(\vec{\sigma}_2 \cdot \vec{k}) \\ O_4 &= \tfrac{i}{2}(\vec{\sigma}_1 + \vec{\sigma}_2) \cdot \vec{n}, \\ O_5 &= (\vec{\sigma}_1 \cdot \vec{n})(\vec{\sigma}_2 \cdot \vec{n}), \end{aligned} \tag{7.19}$$

where $\vec{k} = \vec{q}' - \vec{q}$, $\vec{n} = \vec{q} \times \vec{q}' \equiv \vec{P} \times \vec{k}$ and $\vec{P} = \frac{1}{2}(\vec{q} + \vec{q}')$ is the average momentum. The potential forms $V_i$ are then functions of $\vec{k}$, $\vec{P}$, $\vec{n}$ and the energy. In order to perform a non-relativistic reduction, usually the energy $E$ is expanded in $\vec{k}^2$ and $\vec{P}^2$

$$E(\vec{q}) = \left( \frac{\vec{k}^2}{4} + \vec{P}^2 + M^2 \right)^{\frac{1}{2}} \simeq M + \frac{\vec{k}^2}{8M} + \frac{\vec{P}^2}{2M}. \tag{7.20}$$

and terms to leading order in $\vec{k}^2/M^2$ and $\vec{P}^2/M^2$ are taken into account. The meson propagators $D_\alpha(k^2)$ given in Eq. (**??**) are approximated by their static form $(-1)/(\vec{k}^2 + m^2)$. The equivalent to Eq. (**??**) in configuration space is given by

$$\begin{aligned} O_1 &= 1, \\ O_2 &= \vec{\sigma}_1 \cdot \vec{\sigma}_2, \\ O_3 &= S_{12} = 3(\vec{\sigma}_1 \cdot \hat{\vec{r}})(\vec{\sigma}_2 \cdot \hat{\vec{r}}) - \vec{\sigma}_1 \cdot \vec{\sigma}_2, \\ O_4 &= \vec{L} \cdot S, \\ O_5 &= Q_{12} = \tfrac{1}{2}[(\vec{\sigma}_1 \cdot \vec{L})(\vec{\sigma}_2 \cdot \vec{L}) + (\vec{\sigma}_2 \cdot \vec{L})(\vec{\sigma}_1 \cdot \vec{L})]. \end{aligned} \tag{7.21}$$

These operators are the well known central, spin-spin, tensor, spin-orbit and quadratic spin-orbit operators, respectively. The total angular momentum is denoted by $\vec{L} = \vec{r} \times \vec{P}$ and the total spin $\vec{S} = \frac{1}{2}(\vec{\sigma}_1 + \vec{\sigma}_2)$.

## 7.4 The T-matrix in scattering theory

In this subsection we introduce the concept of the T-matrix in scattering theory. For pedagogical reasons we start with non-relativistic scattering theory which leads to the so-called Lippmann-Schwinger equation. Afterwards we turn to relativistic scattering theory and briefly discuss the Bethe-Salpeter equation, the relativistic counterpart of the Lippmann-Schwinger equation.

### 7.4.1 The Lippmann-Schwinger equation

Let's start with the free Schrödinger equation, given by

$$(E - H_0)\phi = 0 \ ,$$

where $H_0$ is the free Hamiltonian. If there exists an external potential, we have

$$(E - (H_0 + V))\psi = (E - H)\psi = 0$$

In the simplest case this describes the scattering of *one* particle in an external potential $V$, e.g. the scattering of an electron in the electromagnetic potential of an atom or the scattering of a nucleon in the potential of a nucleus. The same formalism van, however, be used for the description of two-body scattering. $V(r)$ corresponds then to the two-body potential which depends on the relativ coordinate $r$ and the scattering problem has to formulated in the center-of-mass frame of the two particles. The Hamiltonian is then given by

$$H = H_0 + V = -\frac{\hbar^2}{2\mu}\nabla^2 + V(r) \ . \tag{7.22}$$

The mass which appears in Eq. (7.17) is the *reduced mass*

$$\mu = M_1 M_2/(M_1 + M_2) \tag{7.23}$$

of particle one and two and $\psi$ describes the relative wave function of particle one and two. The Green function for the free wave function which corresponds to the Eigenvalue $E$ is defined by

$$G_0^+ = \frac{1}{E - H_0 + i\epsilon} \ .$$

In the case of an additional potential we have

$$G^+ = \frac{1}{E - H + i\epsilon}$$

which solves the Schrödinger equation

$$\left[E + \frac{\hbar^2}{2\mu}\nabla^2 + V(r)\right] G^+(\vec{r},\ \vec{r}\,') = \delta^{(3)}(\vec{r} - \vec{r}\,') \ .$$

The explicit form of $G^+$ is

$$G^+(\vec{r},\ \vec{r}\,') = \frac{1}{(2\pi)^3} \int d^3k' \, \frac{\psi_{\vec{k}\,'}(\vec{r})\ \psi^*_{\vec{k}\,'}(\vec{r}\,')}{E - E' + i\epsilon} \ .$$

Analysing the free Green function one finds that it can be decomposed into a real part given by the principal value of the propagator and a purely imaginary part:

$$G_0 = \frac{1}{E - H_0 + i\epsilon} = P\frac{1}{E - H_0} - \pi i \delta(E - H_0) \ .$$

The total wave function can be written as the sum of the incoming free wave function $\Phi$ and scattered wave function $\Psi$, both belonging to the same Eigenvalue $E$. Thus we can write

$$(E - H)\Psi = (E - H_0)\Phi$$

which is equal to

$$(E - H_0)\Psi = (E_0 - H_0)\Phi + V\Psi \ .$$

Therefore the scattered wave function becomes

$$\boxed{\Psi_{\vec{k}} = \Phi_{\vec{k}} + \frac{V}{E - H_0 + i\epsilon}\Psi_{\vec{k}}} \tag{7.24}$$

which is the so-called *Lippmann-Schwinger* equation. An iteration of the Lippmann-Schwinger equation leads to the Born series

$$\Psi_{\vec{k}} = \Phi_{\vec{k}} + \frac{1}{E - H_0 + i\epsilon}V\Phi_{\vec{k}} + \frac{1}{E - H_0 + i\epsilon}V\frac{1}{E - H_0 + i\epsilon}V\Phi_{\vec{k}} + \cdots \ .$$

By inserting a plain wave ansatz $\Phi_{\vec{k}} = e^{i\vec{k}\vec{r}}$, the first part of the Lippmann-Schwinger equation, i.e. the first term which is linear in the potential $V$, yields the so-called *Born approximation* of scattering theory.

We will now illustrate an important problem which occurs in the perturbative expansion of the scattering problem:

In QCD, the potential is proportional to the running coupling constant $V \propto \alpha^2$ which is small in the perturbative regime of QCD, i.e. $\alpha << 1$. Therefore the perturbative expansion converges fast. In contrast, if we regard strong interaction in the non-perturbative low energy regime of nuclear interaction, V is proportional to the meson-nucleon couplings $g_\mu^2$. As we have seen before, these couplings are large, i.e. $g_\mu^2 \geq 1$. Consequently, a perturbation expansion is not possible and one has to sum the full series in powers of $V$ in the Lippmann-Schwinger equation (7.19).

An useful method to perform this summation in a economical way is to shift the perturbation expansion from the wave function into the interaction. This leads to the introduction of the T-matrix. The T-matrix is defined by

$$T\Phi_{\vec{k}} = V\Psi_{\vec{k}} \ .$$

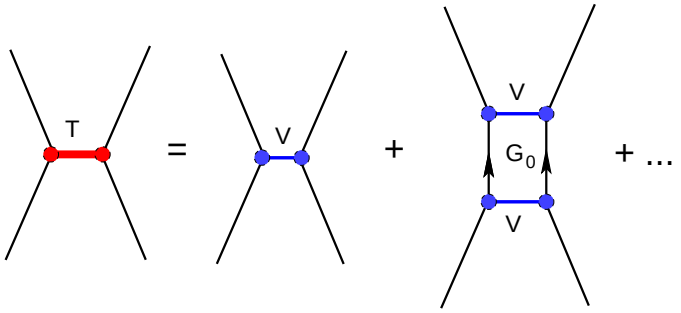


Figure 7.8: Diagrammatic representation of the t-matrix scattering equation.

Inserting this definition into the Lippmann-Schwinger equation one obtains

$$T\Phi_{\vec{k}} = V\Phi_{\vec{k}} + \frac{V^2}{E - H_0 + i\epsilon}\Psi_{\vec{k}}$$

and

$$\boxed{T = V + V\frac{1}{E - H_0 + i\epsilon}T}\,. \tag{7.25}$$

The T-matrix provides an exact solution of the scattering process. Analogous to the Lippmann-Schwinger equation the equation for the T-matrix is an implicit integral equation which is equivalent to the summation of an infinite series of so-called *ladder-diagrams*. This is illustrated in Fig. 7.8.
Up to now, Eqs. (7.19) and (7.20) where written in a schematic way as matrix equations. To evaluate these equations one has to keep in mind that these are integral equations for the matrix elements. E.g. the explicit form of Eq.(7.20) reads

$$\boxed{T(\vec{k},\ \vec{k}\,') = V(\vec{k},\ \vec{k}\,') + \frac{2\mu}{\hbar^3(2\pi)^3}\int d^3k''\,\frac{V(\vec{k},\ \vec{k}\,'')T(\vec{k},\ \vec{k}\,'')}{\vec{k}^{\,2} - \vec{k}\,''^2 + i\epsilon}} \tag{7.26}$$

where matrix elements are given by:

$$T(\vec{k},\ \vec{k}\,') = \left\langle \Phi_{\vec{k}\,'} \right| T \left| \Phi_{\vec{k}} \right\rangle\ .$$

The T-matrix provides the scattering amplitude $f(\vartheta)$, where $\vartheta$ is the scattering angle between the states $\vec{k}$ and $\vec{k}\,'$. It can further be written as the transition matrix element between the incoming free wave $\Phi_{\vec{k}\,'}$ and the outgoing scattered wave $\Psi_{\vec{k}}$:

$$T(\vec{k},\ \vec{k}\,') = -\frac{4\pi\hbar^2}{2\mu}f(\vartheta) = \left\langle \Phi_{\vec{k}\,'} \right| V \left| \Psi_{\vec{k}} \right\rangle\ .$$

This relation leads also to the *optical theorem* which connects the total cross section and the forward scattering amplitude $f(\vartheta = 0)$

$$\boxed{\frac{4\pi}{k}\, Im\, f(0) = \int d\Omega\ |f(\vartheta)|^2 = \sigma_{tot}}\ .$$

---

**Proof of the optical theorem:**

We start with the complex conjugated of Eq. (7.20)

$$T^+ = V + T^+ \frac{1}{E - H_0 - i\epsilon} V \quad .$$

One has to keep in mind that the potential $V$ is fully real whereas $T$ is imaginary. The real and imaginary parts of the $T$ are proportional to the corresponding real and imaginary parts of the propagator (7.4.1). Subtracting the $T^+$ from $T$ only the imaginary parts survive

$$T - T^+ = -2\pi i\, T^+ \delta(E - H_0) T = 2i\, Im\, T\ .$$

Now, the total cross section can be defined by the imaginary part of the T-matrix

$$\sigma_{tot} = \int d\Omega\ |f(\theta)|^2 = \frac{4\pi}{k^2} \sum_{l=0}^{\infty} (2l+1) \sin\delta_l = \frac{4\pi}{k}\, Im\, f(0) = -\frac{2\mu}{\hbar^2 k^2}\, Im\, T(\vec{k},\ \vec{k}\,')\ .$$

Next, we regard forward scattering with $\vartheta = 0$ and $\vec{k}\,' = \vec{k}$. The differential cross section has the form

$$\frac{d\sigma}{d\Omega}(\vartheta,\ \varphi) = |f(\vartheta)|^2\ .$$

Inserting the scattering amplitude in a partial wave representation yields

$$f(\theta) = \frac{1}{k} \sum_l (2l+1) e^{i\delta_l} \sin\delta_l\, P_l(\cos\vartheta) = \frac{1}{k} \sum_l (2l+1)\, T_l\, P_l(\cos\vartheta)$$

we obtain

$$\frac{d\sigma}{d\Omega} = \Big(\frac{\mu}{2\pi\hbar^2}\Big)^2 \Big|T(\vec{k},\ \vec{k}\,')\Big|^2 = \Big(\frac{\mu}{2\pi\hbar^2}\Big)^2 \sum_{l,l'} (2l+1)(2l'+1)\, T_l^*\, T_{l'}\, P_{l'}(\cos\vartheta)\, P_l(\cos\vartheta)\ .$$

Now, we can easily show

$$\frac{d\sigma}{d\Omega} \propto |T(\vartheta)|^2 \qquad \text{and} \qquad \sigma_{tot} \propto Im\, T(\vartheta = 0)\ .$$

---

**Definition: phase shift**

Again we consider the solution of the Schrödinger equation for non-relativistic scattering of an incoming plane wave on a central potential.
A plane wave can actually be written as a sum over spherical waves:

$$\varphi_{inc}(r) = e^{ikz} = \sum_{l=0}^{\infty}(2l+1)\, i^l\, j_l(kr)\, P_l(cos\vartheta)$$

where $j_l(kr)$ are the spherical Bessel functions and $P_l(cos\vartheta)$ the Legendre polynomials.
The solution of the spherically symmetric Schrödinger equation is obtained by the superposition of the incoming plane wave $\phi_{inc}$ and the scattered spherical wave function

$$\psi(r) = \varphi_{inc}(r) + f(\vartheta)\frac{e^{ikr}}{r}\ .$$

The scattering amplitude is defined by

$$f(\vartheta) = \frac{1}{2ik}\sum_{l=0}^{\infty}(2l+1)2ie^{i\delta_l}sin\delta_l$$

and the scattering cross section is given by

$$\frac{d\sigma}{d\Omega} = |f(\vartheta)|^2 = \frac{1}{k^2}\sum_{l\,l'}(2l+1)(2l'+1)P_l(\cos\vartheta)P_{l'}(\cos\vartheta)\sin\delta_l\sin\delta_{l'}\cos(\delta_l-\delta_{l'})\ .$$

By applying the orthogonality relation of the Legendre polynomials

$$\int d\Omega\, P_l(\cos\vartheta)P_{l'}(\cos\vartheta) = \frac{4\pi}{2l+1}\delta_{l\,l'}\ ,$$

the total cross section becomes

$$\boxed{\sigma_{tot} = \frac{4\pi}{k^2}\sum_{l=0}^{\infty}(2l+1)\ \sin^2\delta_l}$$

where $\delta_l$ is called a *phase shift*.
Fig. 7.9 shows the phase shifts in low partial waves ($s : L = 0$, $p : L = 1$ and $d : L = 2$) for neutron-proton scattering which have been obtained with a modern high precision OBE potential, the so-called CD-Bonn potential. For the comparison to data, the potential $V$ has to iterated in the Lippmann-Schwinger equation, respectively the equation for the T-matrix. Therefore Fig. 7.9 contains the theoretical results obtained from the T-matrix based on the potential $V$. We see that corresponding data are reproduced with very high accuracy.

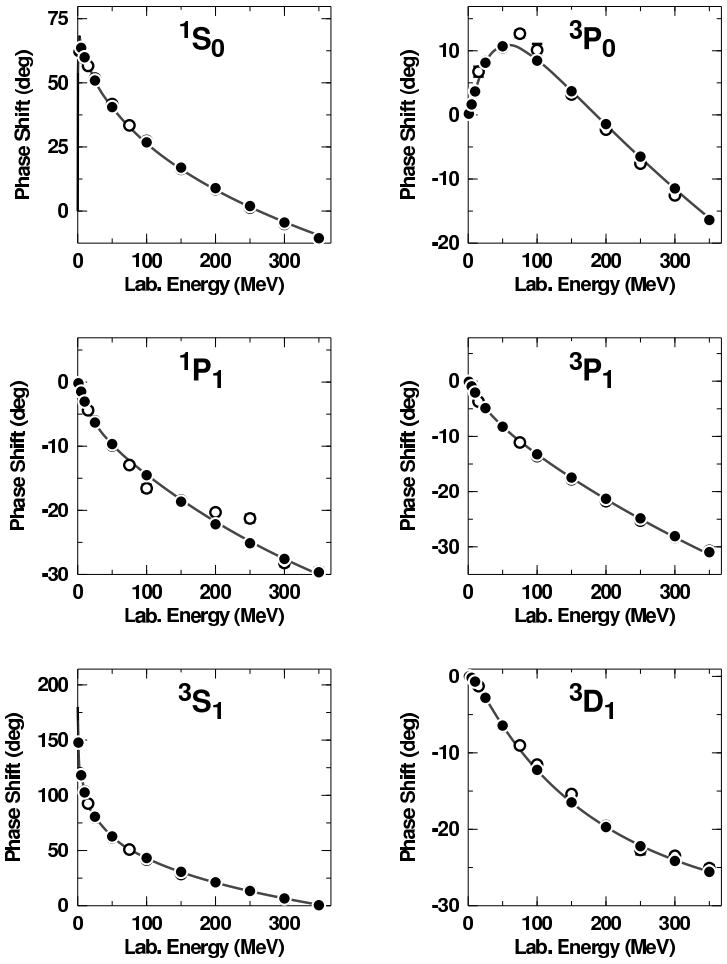


Figure 7.9: Phase shifts in low partial waves for neutron-proton scattering. Experimental analyses (open and solid dots) are compared to the results of a modern high precision OBE potential, the so-called CD-Bonn potential. (The figure is taken from [6].)

### 7.4.2 The Bethe-Salpeter Equation

The relativistic generalisation of the Lippmann-Schwinger equation (7.19), respectively the corresponding equation for the T-matrix (7.20) leads to the so called Bethe-Salpeter Equation (BSE). When one-boson exchange potential are used to describe nucleon-nucleon scattering they have to be inserted into the BSE. E.g. the pahse shifts shown in Figure 7.9 based on a modern version of the Bonn potentials were obtained in this way.
Like in Eq. (7.20) the $\hat{T}$-matrix is defined by

$$\hat{T} = \hat{V} + \hat{V}\hat{G}_2\hat{T} \quad . \tag{7.27}$$

However, Eq. (7.22) is now a matreix equation since $\hat{T}$, $\hat{V}$ and $\hat{G}_2$ are matrices in Dirac-space. $\hat{G}_2 = G_1 G_2$ is the 2-nucleon-propagator where we deonote now explicitely the intermediate states of particle one and two. The scattering process can be again be illustrated by the Feynman-diagrams shown in Figure 7.8.
Rewriting $\hat{T}$ in an expanded form, we obtain the Bethe-Salpeter Equation

$$\boxed{\hat{T}(k',\, k) \;=\; \hat{V}(k',\, k) \;+\; \int \frac{d^4k''}{(2\pi)^3}\, \hat{V}(k',\, k'') \frac{1}{\not{k}'' - M + i\epsilon}\, \frac{1}{\widetilde{\not{k}}'' - M + i\epsilon} \hat{T}(k'',\, k)\;.}$$

The nucleon-propagator is given by

$$G(k) = \frac{1}{k_\mu \gamma^\mu - M + i\epsilon}$$

where

$$k''_\mu = (E'',\, \vec{k}'') \quad \text{and} \quad \widetilde{k}''_\mu = (E'',\, -\vec{k}'')\;.$$

#### The Dirac-Structure of the T-Matrix and Potential

In the following, we study the Lorentz-structure of the T-matrix, contained in the Bethe-Salpeter equation. First, we introduce the two-particle-propagator. In product-space, the two-particle propagator is defined by:

$$\hat{G}_2 = \underbrace{G_1}_{\text{particle 1}} \otimes \underbrace{G_2}_{\text{particle 2}} = \frac{1}{\not{k}'' - M + i\epsilon}\, \frac{1}{\widetilde{\not{k}}'' - M + i\epsilon}\;.$$

By inserting

$$\frac{1}{\not{a} - b} = \frac{\not{a} + b}{(\not{a} - b)(\not{a} + b)} = \frac{\not{a} + b}{\not{a}\,\not{a} - b^2} = \frac{\not{a} + b}{a_\mu a^\mu - b^2}$$

the propagator can be written in the form

$$\begin{aligned} \hat{G}_2 &= \frac{\not{k}'' + M}{k''^{\,2} - M^2 + i\epsilon}\, \frac{\widetilde{\not{k}}'' + M}{\widetilde{k}''^{\,2} - M^2 + i\epsilon} \\ &= \frac{1}{4M^2}\, \frac{\Lambda_1^\dagger(k'')}{k''^{\,2} - M^2 + i\epsilon}\, \frac{\Lambda_2^\dagger(\widetilde{k}'')}{\widetilde{k}''^{\,2} - M^2 + i\epsilon}\;. \end{aligned} \tag{7.28}$$

The operator $\Lambda^+$ projects onto positive energies

$$\Lambda^\dagger_{\alpha\beta}(k) = u_\alpha(\vec{k})\bar{u}_\beta(\vec{k}) = \frac{k_\mu(\gamma^\mu)_{\alpha\beta} + M(\mathbb{1})_{\alpha\beta}}{2M} = \frac{\not{k} + M}{2M}$$

and $\Lambda^-$ onto negative energies

$$\Lambda^-_{\alpha\beta}(\vec{k}) = v_\alpha \bar{v}_\beta \ .$$

(One can easily convince oneself that $\Lambda^\pm$ are indeed projection opertors with $(\Lambda^\pm)^2 = 1$ and $\Lambda^+\Lambda^- = \Lambda^-\Lambda^+ = 0$.)
Therefore, $\hat{G}_2$ is a $8 \times 8$ matrix

$$\hat{G}_2 \propto \left(\begin{array}{c|c} \Lambda^+_1 & 0 \\ \hline 0 & \Lambda^+_2 \end{array}\right) \ .$$

It is the relativistic analog of $G_0$ (7.4.1) which describes the intermediate two-particle state in Eqs. (7.19) and (7.20).
Moreover, $\hat{V}$ and $\hat{T}$ have the same matrix form as $\hat{G}_2$. Consequently, they carry four Dirac-indices.
For example, we have a closer look at $\hat{V}$:

$$\hat{V}_{\alpha\beta,\gamma\delta} = g^2_\mu \quad \underbrace{\bar{u}_\alpha \Gamma_{\beta\sigma} u_\sigma}_{\text{particle 1 (4×4matrix)}} \quad D_\mu \quad \underbrace{\bar{u}_\gamma \Gamma_{\delta\rho} u_\rho}_{\text{particle 2 4×4matrix}}$$

where the meson-propagator $D_\mu$ is a scalar.
Next, we take a second example and only consider the indices of particle 1 in the BS equation

$$T_{\alpha\beta,-} = V_{\alpha\beta,-} + V_{\alpha\sigma,-} G_{\sigma\rho,-} T_{\rho\beta,-} \ .$$

The potentials $V_\mu$ represent scalar- ($\sigma$), pseudo-scalar- ($\pi$), vector- ($\omega$, $\rho$) and tensor-potentials ($\rho$) in Clifford algebra. The two-nucleon-propagator $\hat{G}_2$ is the sum of a scalar and a vector. That's why all components are contained in the $\hat{T}$ matrix

$$\hat{T} = T_S \mathbb{1} \otimes \mathbb{1} \ + \ T_V \gamma_\mu \otimes \gamma^\mu + T_{PS} \gamma_5 \otimes \gamma_5 \ + \ T_T \sigma^{\mu\nu} \otimes \sigma_{\mu\nu} \ + \ T_A \gamma_5 \gamma_\mu \otimes \gamma_5 \gamma_\mu \ .$$

Generally, the determination of the different Lorentz components is difficult.

### 7.4.3 Two-body correlations from the T-matrix

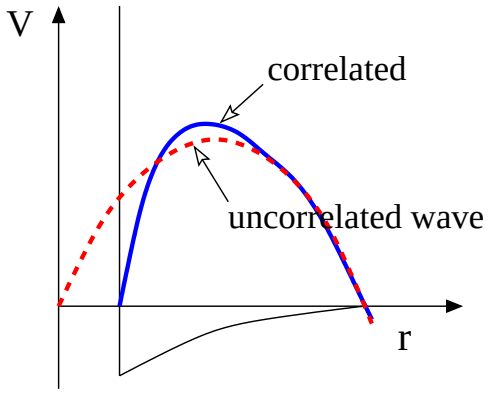


Figure 7.10: Effect of the two-body correlations on the two-nucleon wave function as a function of the relative distance $r$. The nucleon-nucleon potential is schematically indicated. It shows the typical short-range repulsion (hard core) together with the intermediate and long-range attractive parts. The figure is taken from [2].

## 7.5 The Deuteron

The deuteron is the only bound two nucleon state. It consists of a proton and a neutron. Essential parameters which characterise the deuteron, are

- binding energy
- magnetic moment
- quadrapole momentum
- intermediate radius
- charge distribution, probed by electron scattering.

The values are very accurately known from the experimental side. The binding energy of the deuteron is $E_{Bind} = 2.22464$ MeV [2]. which is rather small compared to the average binding energy of about 8 MeV per nucleon in larger nuclei. The deuteron is therefore a rather weakly bound two-nucleon state. Consequently, the size of the deuteron is large, i.e. more than 4 fm. The weak interaction generates a large interaction-radius. This means that the long-range part of the nuclear forces is most important for the description of the deuteron. As we have learned, the long-range part is mainly generated by the one-pion exchange (OPE). We have seen that the strength and even the sign of the various contributions (central and tensor force) of the OPE depend on the quantum numbers $S, I$ and $L$ and are different in spin- and isospin singlet and triplet states.

[2]The binding energy is experimentally known with high precision. It can be measured by photo-induced disintegration of the deuteron $\gamma + d \longmapsto p + n$.

*The deuteron provides an first and important test case for the applicability of the one-boson-exchange picture of the nucleon-nucleon interaction.*

First, we specify the deuteron wave function which is given by

$$d = \frac{1}{\sqrt{2}}(|pn\rangle - |np\rangle) \; .$$

We recall the quantum numbers of the deuteron: The deuteron is an isospin singlet state $I = 0$, but the total spin is $S = 1$. Therefore, there exists a spin triplet state with spin orientations $S_Z = M = -1,\ 0,\ 1$. The total angular momentum is given by $J = 1$. For a fixed angular momentum $L$, there exist two possible spin-orbital couplings

$$\begin{aligned} J = S + L \quad &\Rightarrow \quad L = 0 \\ J = S - L \quad &\Rightarrow \quad L = 2 \; . \end{aligned}$$

The neutron-proton system can be separated into an centre-of-mass part, which behaves like a free (composite) particle, and the part which describes the relative motion of the proton and neutron. The relative wave function is given by $\psi(\vec{r})$. Assuming a central potential, the Schrödinger equation becomes

$$\left[ -\hbar^2 \frac{1}{2\mu} \nabla^2 + V(r) \right] \psi(\vec{r}) = E \, \psi(\vec{r}) \; . \tag{7.29}$$

The mass which appears in Eq. (7.24) is again the reduced mass (7.18) of the two particles. Next, the wave function $\psi(\vec{r})$ is written in a partial wave expansion

$$\psi(\vec{r}) = \frac{1}{kr} \sum_{l=0}^{\infty} \sum_{m=-l}^{l} \frac{u_l(r)}{r} Y_{lm}(\Theta,\ \varphi) \; .$$

By inserting this expression into Eq. (7.24), a differential equation for $u_l$ is obtained

$$\frac{d^2 u_l(r)}{dr^2} + \left[ k^2 - \frac{2\mu}{\hbar^2} V(r) - \frac{l(l+1)}{r^2} \right] u_l(r) = 0 \; . \tag{7.30}$$

Furthermore, we have to take care of the boundary conditions which are determined by the asymptotics.:
For large distances the potential has to vanish, i.e. $r \to \infty$, $V(r) \to 0$ . Consequently, the Schrödinger equation is solved by spherical Bessel $j_l(kr)$ and Neumann $n_l(kr)$ functions.

As we have seen from above, the deuteron wave function contains a $s$-wave ($L = 0$) and a $d$-wave ($L = 2$) component. The $s$-state wave function can be written as

$$\psi^{L=0}_{J=1,\,M} = \frac{1}{\sqrt{4\pi)}} \frac{u(r)}{r} \, \chi_{S=1,\,M_S}$$

where $\chi_{S=1,\,M_S}$ represents the spin part of the wave function. In the spin triplet state, depending on $M_S$, it has the form

$$\chi_{S=1,\,M_S} = \begin{cases} \left|-\frac{1}{2}\ -\frac{1}{2}\right\rangle & M_S = -1 \\ \frac{1}{\sqrt{2}}\left(\left|\frac{1}{2}\ -\frac{1}{2}\right\rangle + \left|-\frac{1}{2}\ \frac{1}{2}\right\rangle\right) & M_S = 0 \\ \left|\frac{1}{2}\ \frac{1}{2}\right\rangle & M_S = +1\ . \end{cases}$$

The interaction potential includes a tensor term. One can show, that a $d$-state ($L = 2$) is generated when the tensor $\hat{S}_{12}$ acts on a $s$-wave function ($L = 0$).
We regard a state, represented by the angular momentum quantum numbers

$$|JM,\ LM_L,\ SM_S\rangle\ .$$

Applying the tensor operator to a L=0 state leads to a d-wave

$$\hat{S}_{12}\,|1M,\ 00,\ 1M\rangle = \sqrt{8}\,|1M,\ 20,\ 1M\rangle\ . \tag{7.31}$$

Now, we can write down the total wave function of deuterium

$$\begin{aligned} \psi &= \psi^{L=0}_{J=1,\,M} + \psi^{L=2}_{J=1,\,M} \\ &= \frac{1}{\sqrt{4\pi}}\left[\frac{u(r)}{r} + \frac{w(r)}{r}\frac{1}{\sqrt{8}}\hat{S}_{12}(\hat{r})\right] |\underbrace{1M,\ 00,\ 1M}_{\equiv\chi_{1\,M}}> \end{aligned}$$

The radial part of the $d$-wave function ($L = 2$) is in the following denoted by $\frac{w(r)}{r}$. The total wave function must be normalised which leads to the normalisation condition

$$\int_0^\infty dr\ \left[u^2(r) + w^2(r)\right] = 1\ .$$

By using this relation and by inserting $k^2 = -ME$, where $E$ is the deuteron binding energy, the radial equation (7.25) becomes with $\hbar = 1$

$$u_l'' = \left[ME + MV_\pi + \frac{l(l+1)}{r^2}\right] u_l\ . \tag{7.32}$$

Assuming that proton and neutron masses are equal $M_p = M_n = M$ the reduced mass is simply $\mu = M/2$ which has been inserted into (7.27). $V_\pi$ in (7.27) is the complete one-pion exchange potential

$$V_\pi = V_c + \hat{S}_{12}(\hat{r})V_T\ .$$

Since the tensor operator in Eq. (7.27) transforms the $s$-wave $u_l$ into a $d$-wave $w_l$, Eq. (7.27) is actually equivalent to two coupled differential equations for $u_l$ and $w_l$:

$$\begin{aligned} L = 0: &\quad u'' = [EM + MV_c]u + \sqrt{8}MV_T\,w \\ L = 2: &\quad w'' = [EM + \tfrac{6}{r^2} + MV_c - 2MV_T]\,w + \sqrt{8}MV_T\,u \end{aligned} \tag{7.33}$$

where $E$ is the binding energy. One can write these two equations (7.28) in a more transparent way if one introduces a matrix notation. To do so we write the total wave function as

$$\psi(r) = \frac{1}{\sqrt{4\pi}} \left[ \frac{u}{r} \begin{pmatrix} 1 \\ 0 \end{pmatrix} + \frac{w}{r} \begin{pmatrix} 0 \\ 1 \end{pmatrix} \right]$$

where the two-dimensional vectors represent $s$ and $d$ wave states
$\begin{pmatrix} 1 \\ 0 \end{pmatrix} \equiv (L = 0)$ and $\begin{pmatrix} 0 \\ 1 \end{pmatrix} \equiv (L = 2)$.
We have learned that the tensor operator $\hat{S}_{12}$ flips the s-wave into a d-wave (see eq. (7.26)), i.e.

$$\hat{S}_{12} \begin{pmatrix} 1 \\ 0 \end{pmatrix} = \sqrt{8} \begin{pmatrix} 0 \\ 1 \end{pmatrix} . \tag{7.34}$$

Finally, the radial equation (7.28) becomes

$$\left[ u'' + \frac{w''}{\sqrt{8}} \hat{S}_{12} \right] \begin{pmatrix} 1 \\ 0 \end{pmatrix} = \left[ EM + MV_c + MV_T \hat{S}_{12} + \frac{6}{r^2} \begin{pmatrix} 0 & 0 \\ 1 & 0 \end{pmatrix} \right] \left[ u + \frac{w}{\sqrt{8}} \hat{S}_{12} \right] \begin{pmatrix} 0 \\ 1 \end{pmatrix}$$

inserting (7.29), the above equation takes the form

$$u'' \begin{pmatrix} 1 \\ 0 \end{pmatrix} + u'' \begin{pmatrix} 0 \\ 1 \end{pmatrix} = [EM + MV_c] u \begin{pmatrix} 1 \\ 0 \end{pmatrix} + [EM + MV_c]\, w \begin{pmatrix} 0 \\ 1 \end{pmatrix}$$
$$+ \frac{6}{r^2} w \begin{pmatrix} 0 \\ 1 \end{pmatrix} + \sqrt{8} MV_T u \begin{pmatrix} 0 \\ 1 \end{pmatrix} + MV_T \frac{w}{\sqrt{6}} \hat{S}^2_{12} \begin{pmatrix} 1 \\ 0 \end{pmatrix}$$

With the relation

$$\hat{S}^2_{12} \begin{pmatrix} 1 \\ 0 \end{pmatrix} = 8 \begin{pmatrix} 1 \\ 0 \end{pmatrix} - 2\sqrt{8} \begin{pmatrix} 0 \\ 1 \end{pmatrix}$$

follows

$$\hat{S}^2_{12} = \begin{pmatrix} 0 & \sqrt{8} \\ \sqrt{8} & -2 \end{pmatrix} .$$

Doing so, the coupled set of equations can now be solved. The results of such a calculation is shown in Fig. 7.10. Fig. 7.10 compares the pure one-pion-exchange calculation to a corresponding calculation which is based on a complete sophisticated nucleon-nucleon potential. In the present case this is the so-called Paris potential which is a high precision non-relativistic potential. In the framework of meson-exchange potentials it would correspond to the inclusion of the other mesons as well. From Fig. 7.10 we see that the $s$-wave function generated by the OPE is very close to that from the full Paris potential. At long distances this is also the case for the $d$-wave function. At short distances also the

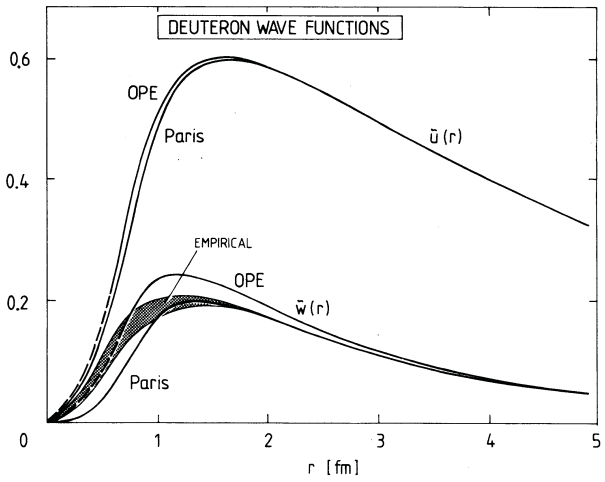


Figure 7.11: $s$- ($u$) and $d$-wave ($w$) deuteron wave functions generated by one-pion-exchange (OPE). The results are compared to a calculation which is based on a full nucleon-nucleon potential (Paris). (The figures are from Ericson and Weise, Pions and Nuclei, Clarendon Press, 1988.)

$d$-wave results are in qualitative agreement. Both are in relatively good agreement with the measured value for the $d$-wave function and, correspondingly, the root-mean-square radii agree also with experiment ($r_d \simeq 4.3$ fm). This demonstrates that the deuteron reflects indeed the properties of the one-pion-exchange potential and that the concept of meson exchange to describe the nuclear forces makes sense.

## 7.6 Survey on modern NN potentials*

### Meson-theoretical potentials

The standard Bonn (A,B,C) potentials [4] contain 13 free parameters for coupling constants and cut-off masses and two additional parameters if one considers the masses of the scalar mesons as effective parameters.

In contrast to the standard Bonn potentials the OPE part of the CD-Bonn potential [6] accounts for charge symmetry breaking in $nn$, $pp$ and $np$ scattering due to the different pion masses $m_{\pi^0}$ and $m_{\pi^\pm}$. The CD-Bonn potential can be referred to as a phenomenological $NN$ potential, since by fine-tuning of the partial wave fits $\chi^2$ per datum is minimised to 1.02, adding up to a total of 43 free parameters.

We consider the modern Nijmegen soft-core potential Nijm93 [5] as the first example of a non-relativistic meson-theoretical potential. It is an updated version of the Nijm78 potential, where the low energy $NN$ interaction is based on Regge-pole theory leading to the well known OBE forces. The contributions considered in this model are the pseudo-scalar

mesons $\pi$, $\eta$, $\eta'$, the vector mesons $\rho$, $\phi$, $\omega$ and the scalar mesons $\delta$, $S^*$, $\epsilon$ and the Pomeron $P$ and the $J = 0$ tensor contributions, leading all in all to a number of 13 free parameters. Since it is constructed from approximate OBE amplitudes it is based on the operator structure given in Eq. (**??**) plus an additional operator $O_6 = \frac{1}{2}(\vec{\sigma}_1 - \vec{\sigma}_2) \cdot \vec{L}$ accounting for charge independence breaking which is new compared to the older version Nijm78. Exponential form factors are used. This potential gives a $\chi^2$ per datum of 1.87, which is comparable to similar OBE potentials like the standard Bonn potentials.

**Phenomenological potentials**

Another class of non-relativistic $NN$ potentials are the so called high quality potentials where $\chi^2/N_{data} \approx 1.0$. Here we study the Nijmegen potentials Nijm I, Nijm II and Reid93 [**?**]. The Nijm I and Nijm II potentials are both based on the Nijm78 potential. In the Nijm I potential some nonlocal terms in the central force are kept whereas in the Nijm II potential all nonlocal terms are removed. Although based on the meson-theoretical Nijm78 potential these potentials are often referred to as purely phenomenological models, since the parameters are adjusted separately in each partial wave leading to a total of 41 parameters. At very short distances, both potentials are regularised by an exponential form factor.
The Nijmegen soft-core Reid93 potential is a phenomenological potential and is therefore based on a completely different approach. In the meson-theoretical Nijmegen potential Nijm93 the potential forms $V_i$ are the same for all partial waves, whereas in the Reid93 potentials every partial wave is parametrised separately by a convenient choice of combinations of central, tensor and spin-orbit functions (local Yukawas of multiples of the pion mass) and the related operators, i.e., the operators $O_1$ to $O_4$ from Eq. (**??**). It is regularised by a dipole form factor and has 50 phenomenological parameters giving all in all a $\chi^2/N_{data} = 1.03$. All the Nijmegen potentials contain the proper charge dependent OPE accounting for charge symmetry breaking in $nn$, $pp$ and $np$ scattering due to different pion masses $m_{\pi^0}, m_{\pi^\pm}$.
The same holds for the Argonne potential $v_{18}$ [**?**], also an example for a widely used modern high precision phenomenological $NN$ potential. It is given by the sum of an electromagnetic (EM) part, the proper OPE, and a phenomenological intermediate- and short-range part unrestricted by a meson-theoretical picture:

$$V = V^{EM} + V^{\pi} + V^{R} \; . \tag{7.35}$$

The EM interaction is the same as that used in the Nijmegen partial-wave analysis. Short-range terms and finite-size effects are taken into account as well [**?**].
The strong interaction part $V^{\pi} + V^{R}$ can be written in a form like given in Eq. (**??**) in configuration space, where the Argonne $v_{18}$ potential is not constructed by approximating the field-theoretical OBE amplitudes (except for the OPE), but by assuming a very general two-body potential constrained by certain symmetries. The potential forms $V_i$ parametrising the intermediate and short-range part are mostly local Woods-Saxon functions.

The local two-body operators are the same charge independent ones used in the Argonne $v_{14}$ potential

$$O_i \;=\; 1, \vec{\sigma}_1\cdot\vec{\sigma}_2, \hat{S}_{12}, \vec{L}\cdot\vec{S}, L^2, L^2(\vec{\sigma}_1\cdot\vec{\sigma}_2), (\vec{L}\cdot\vec{S})^2. \tag{7.36}$$

Due to isovector exchange these operators have to be multiplied by the isospin matrices $\vec{\tau}_1\cdot\vec{\tau}_2$ which than adds up to 14 operators. Additionally, four operators accounting for charge independence breaking are introduced

$$O_{i=15,18} = \hat{T}_{12},\ (\vec{\sigma}_1\cdot\vec{\sigma}_2)\hat{T}_{12},\ \hat{S}_{12}\hat{T}_{12},\ (\tau_{z1}+\tau_{z2})\ , \tag{7.37}$$

where

$$\hat{T}_{12} = 3\tau_{z1}\tau_{z2} - \vec{\tau}_1\cdot\vec{\tau}_2\ \ ,$$

is the isotensor operator, defined analogously to the spin tensor $\hat{S}_{12}$ operator.
Thus the operator structure is more general than that imposed by a non-relativistic, local OBE picture, in particular for the intermediate and short distance part. In total, Argonne $v_{18}$ contains 40 adjustable parameters and gives a $\chi^2$ per datum of 1.09 for 4301 *pp* and *np* data in the range 0–350 MeV [**?**].

### Effective Field Theory (EFT) potentials

A more systematic and direct connection to QCD is provided by chiral effective field theory (EFT). Following the concept originally proposed by Weinberg [**?**] there has been substantial progress in recent time in order to derive quantitative $NN$ potentials from chiral effective field theory (see Chapter XXX).
Up to now the two-nucleon system has been considered at next-to-next-to-next-to-leading order ($\mathrm{N^3LO}$) in chiral perturbation theory [**?**, **?**]. In such approaches the $NN$ potential consists of one-, two- and three-pion exchanges and contact interactions which account for the short-range contributions. The advantage of such approaches is the systematic expansion of the $NN$ interaction in terms of chiral power counting. The expansion is performed in powers of $(Q/\Lambda_\chi)^\nu$ where $Q$ is the generic low momentum scale given by the nucleon three-momentum, or the four-momenta of virtual pions or a pion mass. $\Lambda_\chi \simeq 4\pi f_\pi \simeq 1$ GeV is the chiral symmetry breaking scale which coincides roughly with the Borel mass $\Lambda_B$ of the sum rules. In such an expansion the low-energy constants (LECs) related to pion-nucleon vertices can be fixed from pion-nucleon scattering data. The effective chiral Lagrangian can be written as

$$\mathcal{L}_{\rm eff} = \mathcal{L}^{(2)}_{\pi\pi} + \mathcal{L}^{(1)}_{\pi N} + \mathcal{L}^{(2)}_{\pi N} + \mathcal{L}^{(3)}_{\pi N} + \ldots, \tag{7.38}$$

where the superscript refers to the number of derivatives or pion mass insertions (chiral dimension) and the ellipsis stands for terms of chiral order four or higher. The corresponding chiral $NN$ potential is then defined by

$$V(\vec{q}\,',\vec{q}) \equiv \left\{ \begin{array}{c} \text{sum of irreducible} \\ \boldsymbol{\pi + 2\pi} \text{ contributions} \end{array} \right\} + \text{ contacts}\,. \tag{7.39}$$

The $2\pi$ exchange contributions to the $NN$ interaction at order four have been derived by Kaiser [**?**]. Recently, quantitative $NN$ potentials including contact terms at order four were derived by Entem and Machleidt, the so-called Idaho potential [**?**], and by Epelbaum, Glöckle and Meissner [**?**].
Here we present the Idaho potential [**?**]. The operator structure of the momentum-space $NN$ amplitude has the general form given in Eq. (**??**) with the operators $O_i$ from Eq. (**??**). The potential forms $V_i$ $(i = C, S, T, LS, \sigma L)$ can be expressed as functions of $|(\vec{q}' - \vec{q})|$ and $|\vec{k}|$.
The Idaho potential is regularised by an exponential cut-off

$$V(\vec{q}', \vec{q}) \longmapsto V(\vec{q}', \vec{q})\, \boldsymbol{e}^{-(q'/\Lambda)^{2n}}\, \boldsymbol{e}^{-(q/\Lambda)^{2n}} \tag{7.40}$$

where $\Lambda = 0.5$ GeV in all partial waves. This does not affect the chiral order of the potential, but introduces contributions beyond that order. The total number of free model parameters in the N$^3$LO potential is 29 [**?**].

**Renormalization Group approach to $NN$ interaction**

Recently, another approach has been proposed to arrive at a better model independent understanding of the $NN$ interaction [**?**]. In this approach a low-momentum potential $V_{\text{low k}}$ is derived from a given realistic $NN$ potential by separating the low-momentum part, i.e., by integrating out the high-momentum modes, and using renormalization group (RG) methods to evolve the $NN$ potential models from the full Hilbert space to the low momentum subspace. At a cutoff of $\Lambda = 2.1$ fm$^{-1}$ all the various $NN$ potential models were found to collapse to a model-independent effective interaction $V_{\text{low k}}$.
Since elastic $NN$ scattering data constrains the $NN$ interaction only up to a momentum scale of about 400 MeV, which corresponds to the pion threshold, modern high precision potentials differ essentially in the treatment of the short-range part, as depicted in Fig. **??**. The philosophy behind the RG approach is to replace the unresolved short distance structure by something simpler, e.g. contact terms, without distorting low-energy observables.

---

Fig. **??** displays the diagonal matrix elements $V(\vec{q}, \vec{q})$ in the $^1S_0$ partial wave for the different high precision $NN$ potential models discussed above. Looking at Fig. **??** now immediately the question arises: *Why yield the various NN interaction so different results when they all explain the same scattering data with about the same precision?*.

The reason lies in the short range part of the NN interaction. Free NN scattering data constrain the potential models up to a laboratory energy of $E_{\text{Lab}} \sim 300$ MeV which corresponds to the pion production threshold. This means that a real pion can be produced in the inelastic reaction $NN \mapsto NN\pi$ (do not mix up with the exchange of a virtual pion). It does not mean that to few experimental data are available above the pion threshold. Instead, the opening of in-elasticities leads to severe uncertainties in the theoretical descriptions. Above the pion threshold the measured total cross section has to be disentangled

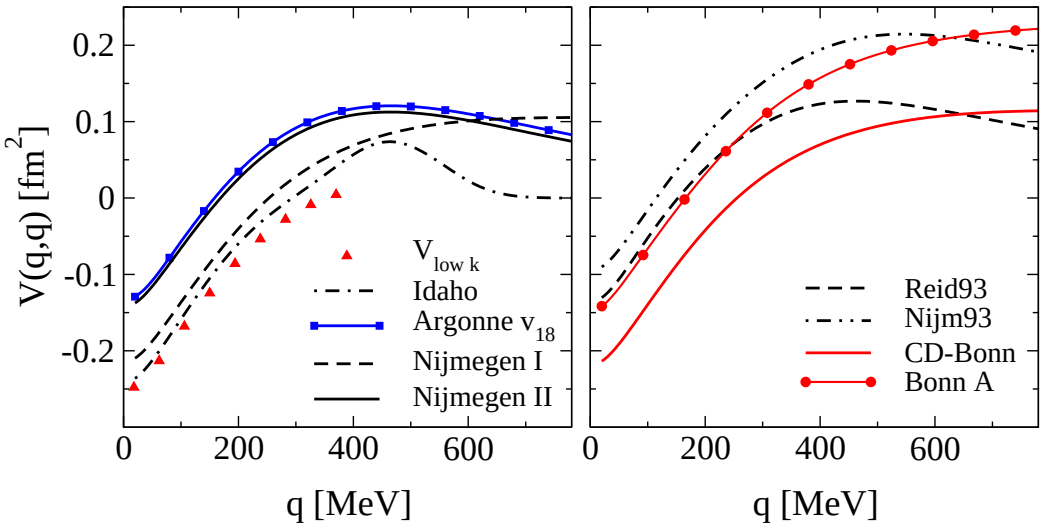


Figure 7.12: Diagonal matrix elements $V(\vec{q},\vec{q})$ in the $^1S_0$ partial wave for different high precision $NN$ potential models.

into elastic and inelastic contributions. This procedure can, however, not be performed with the accuracy necessary to constrain the potentials for elastic scattering sufficiently well.

Thus the scale for a precise determination of the NN interaction is set by the pion threshold. Translated into relative momentum $E_{\rm Lab} \sim 300$ MeV corresponds to

$$|\vec{p}| \sim 400 \text{ MeV} \sim 2 \text{ fm}^{-1} \quad .$$

Translated into coordinate space the 2 fm$^{-1}$ correspond to a relative distance of the wave functions of about 0.5 fm. This is essentially the scale where the hard core of the interaction is operative. Thus the various potentials shown in Fig. **??** differ essentially in the strength of the hard core. Some are more repulsive and some are less. In OBE type models we know that the hard core is mediated by the exchange of the relatively heavy vector mesons $\omega$ and $\rho$ and the strength is proportional to the corresponding coupling constants.

But when the situation is such, does the modulation of the hard core not strongly influence the description of scattering data at lower momenta? The answer is NO. And the reason is that the scattering data are not fitted by the bare potential $\hat{V}$ but by the corresponding T-matrix iterating the Lippmann-Schwinger (7.20) or the Bethe-Salpeter equation (7.22). The T-matrix introduces short-range correlations which suppress the influence of the hard core. This fact is schematically illustrated in Fig. **??** where the relative two-nucleon wave function in coordinate space are shown. While the uncorrelated wave function has full overlap with the hard core, the short-range correlation shift the wave function away from the center and reduce this overlap.

*Quite different NN potentials can lead to identical correlated wave functions.*

# Bibliography


[1] R.J. Furnstahl, Lect. Notes Phys. **641** (2004) 1.

[2] H. Müther, A. Polls, Prog. Part. Nucl. Phys. **45** (2000) 243.

[3] T. Ericson and W. Weise, *Pions and Nuclei*, Clarendon Press, 1988.

[4] R. Machleidt, K. Holinde, Ch. Elster, Phys. Rep. **149** (1987) 1.

[5] V.G.J. Stoks, R.A.M. Klomp, M.C.M. Rentmeester, J.J. de Swart Phys. Rev. C **48** (1993) 792.

[6] V.G.J. Stoks, R.A.M. Klomp, C.P.F. Terheggen, and J.J. de Swart Phys. Rev. C **49**, 2950 (1994).

[7] R. Machleidt, Phys. Rev. C **63** (2003) 024001.

[8] R.B. Wiringa, V.G.J. Stoks, R. Schiavilla, Phys. Rev. C **51**, 38 (1995).

[9] S. Weinberg, Phys. Lett. B **251**, 288 (1990); Nucl. Phys. **B363**, 3 (1991).

[10] D.R. Entem, R. Machleidt, Phys. Rev. C **68**, 041001 (2003).

[11] E. Epelbaum, W. Glöckle, U.-G. Meissner, Nucl. Phys. **A747**, 362 (2005).

[12] S.K. Bogner, T.T.S. Kuo, A. Schwenk, Phys. Rept. **386**, 1 (2003).

[13] O. Plohl, C. Fuchs, Phys. Rev. C **74**, 034325 (2006).

thebibliography